NUMERICAL ANALYSES ON THE STRESS DISTRIBUTION IN COATED SYSTEMS WITH PERPENDICULAR CRACKS UNDER TENSILE LOADS

Cristiane Martins Angelo, cristiane_cma@yahoo.com.br
Newton Kiyoshi Fukumasu, newton.fukumasu@gmail.com
Polytechnic School of the University of Sao Paulo
Av. Prof. Luciano Gualberto, travessa 3 nº 380 - CEP - 05508-900 - São Paulo - SP

Roberto Martins Souza, roberto.souza@poli.usp.br
Polytechnic School of the University of Sao Paulo
Av. Prof. Luciano Gualberto, travessa 3 nº 380 - CEP - 05508-900 - São Paulo - SP

Abstract. *Many techniques exist to characterize the mechanical properties of thin films and coatings. Among these techniques, the conduction of tensile tests on coated specimens is able to provide not only the properties of the film, but also of the film/substrate interface. In this work, a two-dimensional Finite Element Modeling (FEM) analysis was conducted to analyze the stress distribution in coated systems under tensile load, with the presence of two cracks perpendicular to the film/substrate interface. The system was composed of an elastic thin film and of an elastic-plastic substrate and the analysis simulated systems varying the distance between the two cracks along the entire film thickness. Results were analyzed in terms of the distribution of the normal stresses parallel to the loading direction, which confirmed the models available in the literature, including the identification of the sites prone for the occurrence of further film fracture.*

Keywords*: Thin Film, Finite Element Modeling, Tensile Stress, Crack, Fracture.*

1. Introduction

The deposition of films with thickness on the order of micrometers is a common procedure to improve the tribological behavior of mechanical tools and components.

Many techniques exist to characterize the mechanical properties of thin films, which include tensile tests on the entire system, as published by Ignat (2001). In these cases, when the tensile loads are applied on the test specimen, primary cracks randomly propagate perpendicular both to the applied load and film surface. The presence of these primary cracks in the film prevents direct transmission of the tensile load to film regions between two parallel cracks. Then, the entire load must bypass those cracks through the substrate, generating stress concentration fields near the tip of the crack at the interface film/substrate. Accordingly to Latella et. al. (2007), Harry et. al. (1998), Yanaka et. al. (1998) and Hu and Evans (1989), the higher the spacing between two cracks, the higher the stress on the film surface. Besides the point of the highest stress occurs in the middle of the distance between those cracks. Further loading of the system results in further crack propagation and in gradual decrease of the distance between two consecutive cracks, up to a point that no more cracks are nucleated nor propagated. This limiting distance between consecutive cracks is called saturation length. This saturation occurs due to the fact that the stress intensity at the surface of the film is below a critical value (σ_c) needed to nucleate new cracks. Figure 1 shows a periodic distribution of cracks in a film, as presented by Yanaka et. al. (1998) and Fig. 2 shows a schematic of a cracked film with the saturation length between cracks.

In this work, the finite element method (FEM) was used to simulate tensile loads on coated systems with varying distances between two perpendicular cracks, in an effort to further understand the effect of this distance on the saturation length.

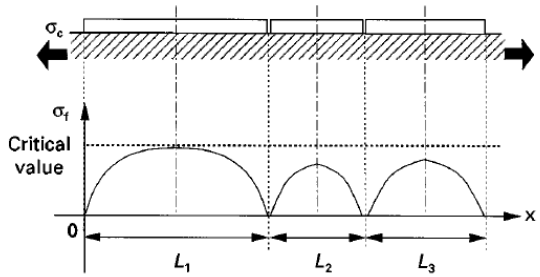

Figure 1. Stress distribution in cracked thin films showing that the higher stress concentration occurs in the middle of two consecutive cracks [Yanaka et. al. (1998)]

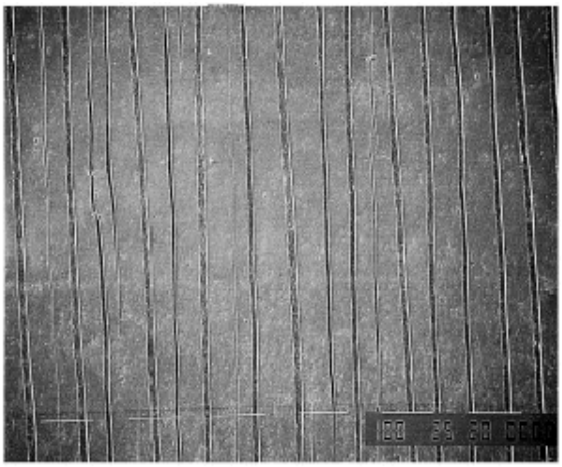

Figure 2. Cracked film with the saturation length between cracks [Harry et. al. (1998)]

2. Model description

2.1. Geometry

Figure 3 presents the geometry analyzed in this work and the main dimensions, which are: film thickness (e), total height (h), length (L) and the distance between two cracks (d). Table 1 presents the values of those parameters selected during the analyses. For all cases, the crack length was defined as equal to e, i.e. the film thickness.

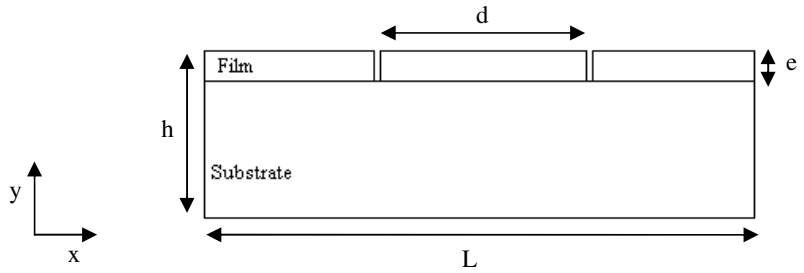

Figure 3. Overall geometry with main parameters: h is the total height, L is the length, d is the distance between two cracks and e is the thickness of the film.

Table 1. Main parameter values selected during the simulations and corresponding cases

Parameter/Case	1	2	3	4	5	6	7	8	9
Ratio d/e	0.5	1	2	3	4	5	10	20	40
Film Thickness (e)	0.0046 mm								
Total Height (h)	0.1 mm								
Lenght (L)	0.38 mm								

2.2. Materials

The mechanical properties selected for the materials were based on Souza (1999). The substrate presented the properties of an aluminum AA6061 alloy in a T6 condition. The properties of the film were defined based on the range usually found for wear resistant films used in coated systems. Those properties are presented in table 2. The film was considered as a linear elastic material. The substrate was defined as a perfectly elastic-plastic material.

Table 2. Mechanical properties for the applied materials

Property	Substrate	Film
Modulus of Elasticity (*E*) [GPa]	68.9	280.0
Poisson's Ratio (ν)	0.3	0.3
Yield Strenght (σ_y) [MPa]	295.0	-

2.3. Crack models

Cracks were modeled as free parallel surfaces in the film and no criterion for crack nucleation or propagation was considered throughout the analysis.

According to Hu and Evans (1989), the stress critical value to nucleate new cracks is given by Eq. 1. Latella et. al. (2007) presented Eq. 2, for the correlation of some properties of the film, like fracture toughness, with the stress critical value to nucleate new cracks.

(1) $\sqrt{3} < \frac{\sigma_y}{\sigma_c}\frac{d}{e} < 2\sqrt{3}$

(2) $\frac{k_{Ic}}{\sigma_c} = \left[\sqrt{3}\frac{\sigma_c}{\sigma_y}e + \pi e F(\frac{E_{film}}{E_{substrate}})\right]^{\frac{1}{2}}$

In Eq. 2, k_{Ic} is the fracture toughness of the film and the term $F(\frac{E_{film}}{E_{substrate}})$ is a function dependent on the ratio between the elastic moduli of the materials and the type of load applied in the system. As presented by Hu and Evans (1898), for a tensile load perpendicular to the cracks, and for a ratio $\frac{E_{film}}{E_{substrate}}$ equal to 4, the value of this function is approximately 0.79.

2.4. Simulation

The finite element method was applied to obtain the distribution of the normal stresses parallel to the applied load. The Abaqus® software from Dassault Systemès Inc. was used to model and resolve the systems. Approximately 400.000 rectangular elements were used to represent the substrate and the film and, almost, 70% of these elements were concentrated near the crack surfaces, to improve the solution at those locations. Figure 4 shows the mesh distribution for the region near the crack. The center of the first element was mapped to be in a distance of 0.012 μm from the interface between the film and the substrate.

The geometry was considered as a 2D body and to solve the stress state at every element, from Fig 1, it was applied the plane strain theory, since this would better represent the conditions found in practice. Due to the large refinement applied near the crack tip, quarter-point elements were not needed to improve the robustness the solution of the problem.

In terms of the boundary conditions, an uniaxial load was applied perpendicular to the cracks at the boundaries of the body with a effective displacement of 1μm. Boundary conditions also restricted the movement of the nodes at the bottom of the mesh in the direction perpendicular to the applied load.

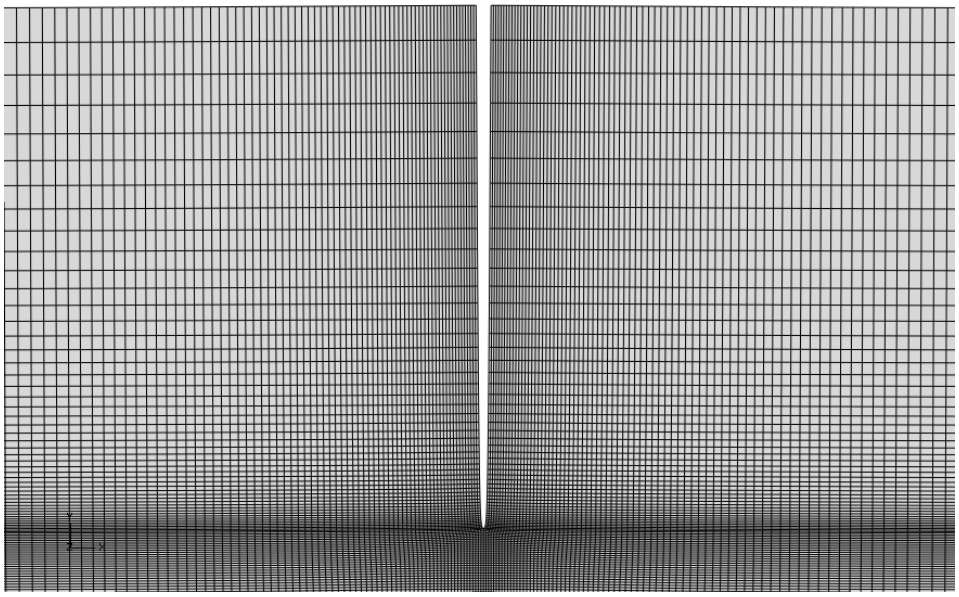

Figure 4. Distribution of the elements in the mesh for one characteristic crack.

3. Results

Figure 5 shows distribution of normal stresses (σ_{11}) parallel to loading direction, both along the film and the substrate. Note that only a detail of the FEM mesh is shown in each case and that film portion in the figure was gradually reduced in order to slow the stresses associated with both cracks, although film thickness was kept constant. As expected, Fig. 5 indicates regions of stress concentration at the tip of each crack. In these cases, the stress fields are compatible with those usually seen at superficial cracks. Figure 5a was calculated for the condition where the distance between cracks was equal to half of the film thickness of the film. In this case, the stress concentration on the substrate due to the existence of two cracks in the film is similar to the existence of only one crack.

Figure 6 shows the stress distribution (σ_{11}) at the surface of the film between the cracks. The shape of this figure is compatible with the ones presented on figure 8, by Harry et. al. (1998), for d/e values higher than 10, except for the compressive stresses close to the cracks (x=0 and x=1), accordingly to results presented by Song et. al. (2006). This compressive stress tends to bend the film at the surface of the crack, trying to separate the film from the substrate at its interface. As this separation is not allowed, the compressive stress was expected. Also from this figure, it is shown that the maximum compressive stress at the surface of the film was reached for d/e equal to 2. Below this value, the stress tends to zero at the film surface between cracks. As shown in Figure 5, when the distance between cracks is almost negligible, the two cracks act like if only one crack was present in the film.

Figure 7 presents the maximum values of σ_{11} , as a function of the ratio d/e, for the conditions at which the peak in σ_{11} was tensile. From this figure, for values d/e higher then 10, the stress σ_{11} tends assintotically to the highest value, which would imply possible superation of the stress critical value and, in practice, the nucleation of new cracks. For values of d/e lower then 10, the system presents a sharp decrease in the stress values, meaning that no new cracks would nucleate. Then the value of 10 times the film thickness for the distance between the cracks could be defined as the saturation length for the system analyzed in this work.

Using Eq. 1 with the saturation length of d/e equal to 10, the stress critical value would be 442 MPa and, from Eq. 2, a fracture toughness on the order of 5 MPa $\sqrt{m}$ would be obtained, which is compatible with the value of many ceramic materials.

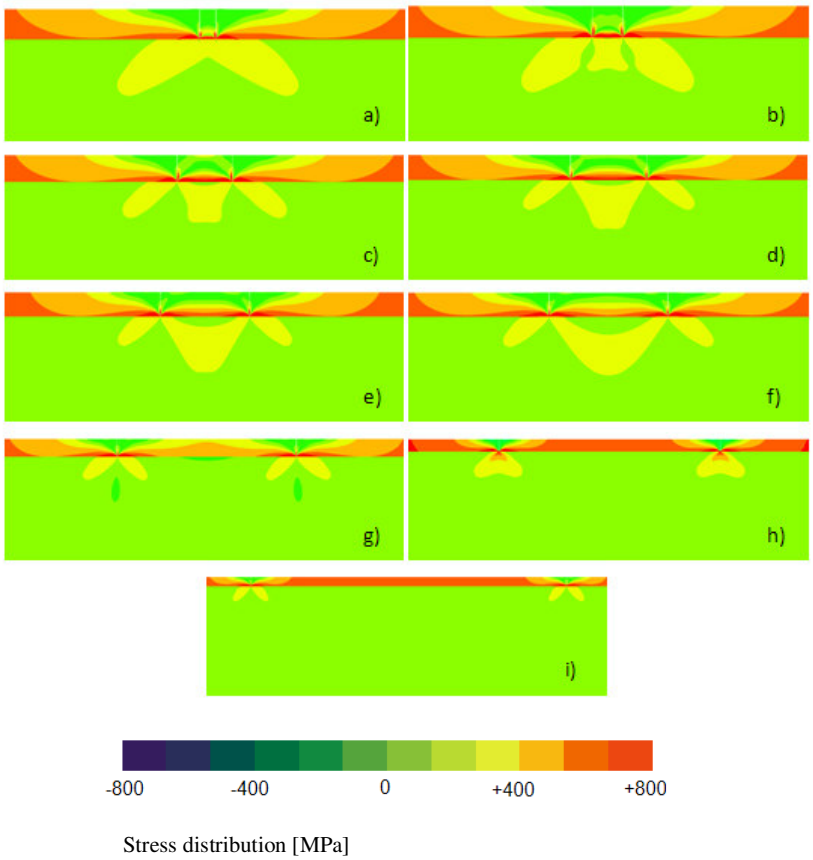

Figure 5. Stress distribution σ_{11} on the region between cracks for the ratio d/e: 0,5 (a); 1 (b); 2 (c); 3 (d); 4 (e); 5 (f); 10 (g); 20 (h); 40 (i)

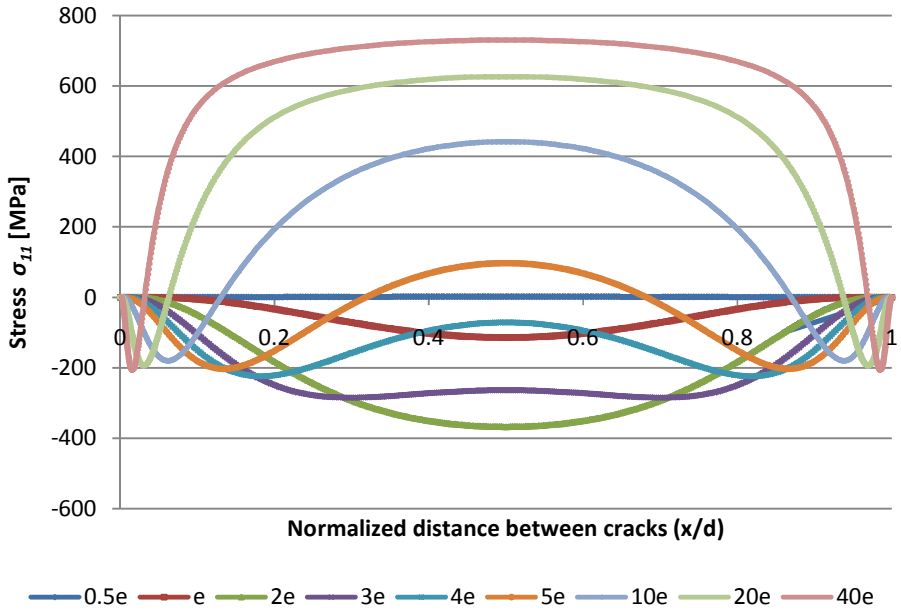

Figure 6. Stress distribution σ_{11} on the film surface for the region between cracks

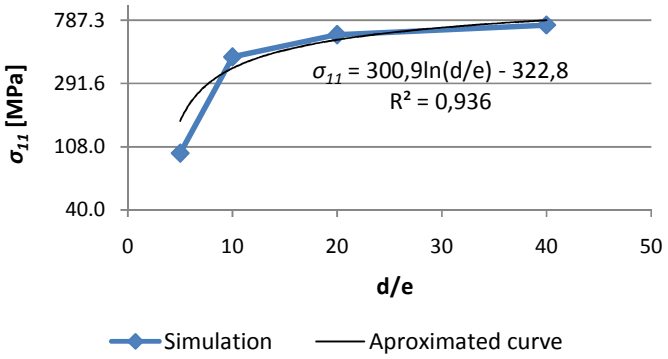

Figure 7. Maximum values for σ_{11} as a function of the ratio d/e

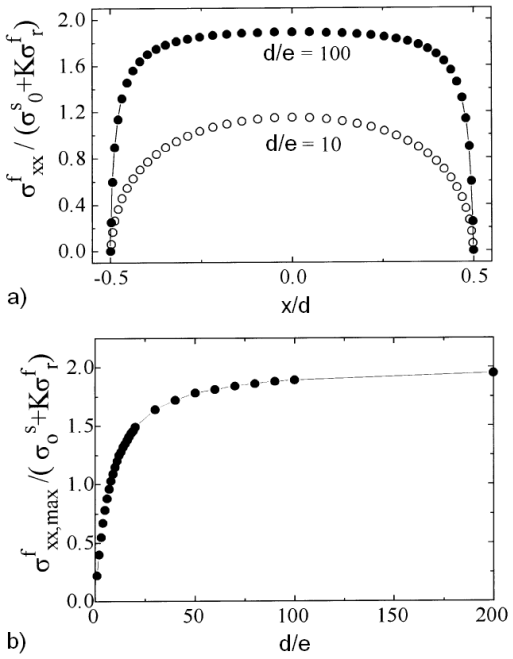

Figure 8. (a) Distribution of normal stress on the film surface between two consecutive cracks; (b) Maximum values for the normal stress as a function of the ratio d/e. Source Harry et. al. (1998).

4. Conclusions

The results presented in this work showed that there is a length between two parallel cracks that, below this value, no new cracks can be nucleated at the surface on a thin ceramic film. This occurs since the stress at the film surface does not reach a critical value, needed to nucleate new cracks, as demonstrated by Latella et. al. (2007), Harry et. al. (1998) and Hu and Evans (1989).

In this work, for the system analyzed, a saturation length of 10 times the film thickness would be expected. For values below d/e equal to 10, the stress distribution on the film surface would probably not reach the stress critical value needed to nucleate new cracks.

For very small distances between cracks, the two cracks acted like one for the stress concentration in the substrate, and as the distance between cracks increases, the influences of each crack in another on the stress concentration in the substrate decreased, until a condition of no mutual influence for large values of d/e.

5. References

Harry, E., Rouzaud, A., Ignat, M., Juliet, P. (1998) Mechanical properties of W and W(C) thin films: Young's modulus, fracture toughness and adhesion. Thin Solid Films, 195-201.

Hu, M.S., Evans, A.G. (1989) The cracking and decohesion of thin films on ductile substrates. Acta Metall, 37, 917-925.

Ignat, M. (2001), Chemical Vapor Deposition, Chapter 3 (Stresses and Mechanical Stability of CVD Thin Films), ASM International, Vol. 2, 45-80.

Latella, B.A., Triani, G., Zhang, Z., Short, K.T., Bartlett, J.R., Ignat, M. (2007) Enhanced adhesion of atomic layer deposited titania on polycarbonate substrates. Thin Solid Films, 3138-3145.

Song, G. M., Sloof, W. G., Pei, Y. T., De Hosson, J. Th. M. (2006) Interface fracture behavior of zinc coatings on steel: Experiments and finite element calculations. Surface & Coatings Technology, 201, 4311-4316.

Souza, R.M. (1999) Finite element modeling of contact stresses during indentation of wear resistant coatings on soft substrates. Tese de doutorado, Escola de Minas do Colorado, EUA.

Yanaka, M., Tsukahara, Y., Nakaso, N., Takeda, N. (1998) Cracking phenomena of brittle films in nanostructure composites analysed by a modified shear lag model with residual strain. Journal of Materials Science, 33, 2111-2119.

6. Responsibility notice

The authors are the only responsible for the printed material included in this paper.

6. Acknowledgements

The authors are grateful for the financial support by the "Conselho Nacional de Desenvolvimento Científico e Tecnológico – CNPq" and for the resources of the Surface Phenomena Laboratory - LFS - at the Polytechnic School of University of Sao Paulo.